Chemical Studies on Antioxidant Mechanism of Curcumin: Analysis of Oxidative Coupling Products from Curcumin and Linoleate

Toshiya Masuda,*[,†] Tomomi Maekawa,[‡] Kayo Hidaka,[‡] Hiromi Bando,[†] Yoshio Takeda,[†] and Hidemasa Yamaguchi[‡]

Faculty of Integrated Arts and Sciences, University of Tokushima, Tokushima 770-8502, Japan, and Graduate School of Human Life Science, Osaka City University, Osaka 558-8585, Japan

As a part of a research project on the antioxidant mechanism of natural phenolics in food components, curcumin, a turmeric antioxidant, was investigated in the presence of ethyl linoleate as one of the polyunsaturated lipids. During the antioxidation process, curcumin reacted with four types of linoleate peroxyl radicals. Six reaction products were observed in the reaction and subsequently isolated. Their structures were determined by physical techniques, revealing that they have novel tricyclic structures, including a peroxyl linkage. On the basis of the formation pathway for their chemical structures, an antioxidant mechanism of curcumin in polyunsaturated lipids was proposed, which consisted of an oxidative coupling reaction at the 3′-position of the curcumin with the lipid and a subsequent intramolecular Diels−Alder reaction.

Keywords: *Curcumin; linoleate; antioxidant mechanism; radical termination; oxidative coupling; structure determination; tricyclic compound*

INTRODUCTION

Curcumin is the main yellow pigment of a popular spice, turmeric, and is widely used as a food colorant (*1*). Curcumin has a potent antioxidant activity (*2*, *3*) and has received attention as a promising nutraceutical or a component of designer foods for its cancer-preventing ability (*4*). Various curcumin-related phenols have also been found in edible or medicinal plants, especially in Zingiberaceae (*5*−*10*). Curcumin has a unique conjugated structure including two methoxylated phenols and an enol form of β-diketone, and the structure shows a typical radical trapping ability as a chain-breaking antioxidant. (Figure 1) The antioxidant mechanism of curcumin has attracted much attention (*11*−*13*); however, it is still not yet well understood. Generally, the nonenzymatic antioxidant process of the phenolic material is thought to be divided into the following two stages:

$$S{-}OO^{\bullet} + AH \rightleftarrows SOOH + A^{\bullet} \quad (1)$$

$$A^{\bullet} + X^{\bullet} \rightarrow \text{nonradical materials} \quad (2)$$

where S is the substance oxidized, AH is the phenolic antioxidant, $A^{\bullet}$ is the antioxidant radical, and $X^{\bullet}$ is another radical species or the same species as $A^{\bullet}$ (*14*). Although the first stage is a reversible process, the second stage is irreversible and must produce stable radical terminated compounds. The structural elucidation of such terminated compounds would afford an important contribution to understanding the mechanism of the phenolic antioxidant. During the course of an antioxidant mechanism study of curcumin, we recently showed that dimerization was a main termination process of the radical reaction of curcumin itself (*15*). On the other hand, in the food system, the antioxidant coexists with a large amount of oxidizable biomolecules such as polyunsaturated lipids. It is well-known that these biomolecules produce reactive peroxyl radicals during their oxidation, which may act as $X^{\bullet}$ and couple with the antioxidant radical ($A^{\bullet}$) in the second step of the above-mentioned antioxidation scheme. We have been investigating the termination stage of the antioxidation process of curcumin in the presence of a lipid. We have now succeeded in isolating the radically coupled products of curcumin and a lipid, ethyl linoleate. In this paper, we report the determination of their chemical structures and the proposed antioxidant mechanism of curcumin in the lipid on the basis of their chemical structures.

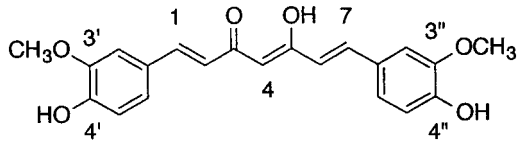

Figure 1. Chemical structure of curcumin.

MATERIALS AND METHODS

Chemicals and Instruments. Curcumin was synthesized using a previously reported method (*16*). 2,2′-Azobis(isobutyronitrile) (AIBN) was obtained from Tokyo Kasei (Tokyo. Japan). Ethyl linoleate was obtained from Kanto (Tokyo, Japan) and used after purification by silica gel (silica gel 60, Merck, Darmstadt, Germany) chromatography developed with 2.5% ethyl acetate in hexane to remove its hydroperoxides. Silica gel TLC plates (silica gel 60 F254 PLC plates) and silica gel for column chromatography (silica gel 60) were purchased from Merck. All solvents and other reagents were obtained from Nacalai (Kyoto, Japan). NMR spectra were measured with a Unity Plus 500 spectrometer (Varian, Palo Alto, CA)

* Author to whom correspondence should be addressed (fax +81-88-656-7244; e-mail masuda@ias.tokushima-u.ac.jp).
† University of Tokushima.
‡ Osaka City University.

10.1021/jf001442x CCC: $20.00
Published on Web 04/17/2001

using the manufacturer-supplied pulse sequences, ^{1}H, ^{13}C, correlated spectroscopy (COSY), nuclear Overhauser effect spectroscopy (NOESY), heteronuclear multiple-quantum correlation (HMBC), and totally correlated spectroscopy (TOCSY). Mass spectra were measured with an SX-102A spectrometer (JEOL, Tokyo, Japan) in the negative FAB mode. IR spectra were measured with an FTIR 1720 spectrometer (Perkin-Elmer, Yokohama, Japan). An LC 6A system (Shimadzu, Kyoto, Japan) equipped with a photodiode array detector (Shimadzu, SPD-M10AP) and a Gulliver Gradient LC system (JASCO, Tokyo, Japan) were used for HPLC. A medium-pressure pump 91-M-8 (Chemco, Osaka, Japan) was used for medium-pressure liquid chromatography (MPLC).

Analysis of Radical Reaction Products. To 3 g of ethyl linoleate in a 40 mL straight vial (40 mm, diameter) were added curcumin (3 mg) in dimethyl sulfoxide (200 μL) and AIBN (600 mg) in CH_3CN (3 mL). The solution was well stirred and then incubated at 40 °C in air. At 1 or 1.5 h intervals, a 100 μL aliquot was removed and diluted with CH_3CN (200 μL). Ten microliters of the diluted solution was injected into the analytical HPLC system under the following conditions: column, Develosil CN-5 (4.6 × 250 mm, Nomura Chemical, Seto, Japan); solvent system, 2% CH_3CO_2H in *n*-hexane (solvent A) and 2% CH_3CO_2H in ethyl acetate (solvent B); elution, linear gradient from 14% of solvent B to 71% of solvent B for 20 min and then isocratic mode of 100% of solvent B for 5 min; flow rate, 2 mL/min; detection, 420 nm. The peak area was calculated using a Shimadzu M-10A data analyzing system. The control experiment was also carried out by the addition of 3.4 mL of CH_3CN instead of 3 g of ethyl linoleate.

Analysis of Hydroperoxide of Ethyl Linoleate. At 1 h intervals, a 10 μL aliquot was removed and then diluted with 5 mL of methanol. Ten microliters of the diluted solution was analyzed by high-performance liquid chromatography (HPLC) under the following conditions: column, YMC ODS-A (4.6 × 150 mm, YMC, Kyoto, Japan); solvent system, 90% CH_3CN in H_2O; flow rate, 1 mL/min; detection, 235 nm. Peak area was calculated using a Shimadzu CR-6A integrator. The hydroperoxide concentration was calculated from the obtained peak area using a calibration curve [$Y = 7.8 \times 10^{-7}X - 0.015$; Y is the amount of ethyl linoleate hydroperoxide (nmol) and X is the observed peak area (range for $X = (3-13) \times 10^5$)] obtained using pure ethyl linoleate hydroperoxide (*17*). The control experiment was carried out using the same procedure and analytical method without curcumin.

Isolation Procedure for Compounds 1−6. The reaction vials, which were prepared according to the above-mentioned procedure, were incubated at 40 °C in air for 4 h. The vials were stored in a freezer at −20 °C overnight, and the precipitate produced was removed by decantation. The supernatant obtained was cooled at −28 °C to freeze the ethyl linoleate, and the supernatant produced was collected. The precipitate was dissolved in 3 mL of CH_3CN and then cooled again at the same temperature to collect the next supernatant. This procedure was repeated twice, and all supernatants were combined and evaporated in vacuo. The residue, which was obtained from five vials, was dissolved in a small amount of CH_2Cl_2 and then injected into the MPLC under the following conditions: column, Develosil LOP-CN 24S (24 × 300 mm); solvent, 20% ethyl acetate in hexane containing 0.2% acetic acid; flow rate, 10 mL/min; detection, 360 nm. The solution eluting from 40 to 55 min was collected and evaporated. The residue obtained was next purified by preparative HPLC using an octadecyl silica gel column to separate compounds **1**−**6** [separation conditions: column, Daisopak ODS-5-AP (20 × 250 mm, Daiso, Osaka, Japan); solvent, 85% CH_3CN in H_2O; flow rate, 16 mL/min; detection, 420 nm]. These procedures was repeated 34 times, and a total of 510 mg of curcumin was treated. Each compound obtained was finally purified for its structure analysis by silica gel TLC developed with ethyl acetate/hexane = 1:2 (isolation yields: 4.7 mg for **1**, 5.1 mg for **2**, 6.9 mg for **3**, 2.6 mg for **4**, 4.4 mg for **5**, and 2.2 mg for **6**).

Analytical Data for Compounds 1—6. *Compound **1***: HRMS-FAB (negative) (*m*/*z*) [M − H]$^-$ calcd for $C_{41}H_{53}O_{10}$ 705.3639, found 705.3651; FAB MS (negative), *m*/*z* 705, 577, 557, 455, 427; IR (dry film), ν_{max} 3409 (OH), 1730 (ester CO), 1703 (CO), 1630 (conjugated CO) cm^{-1}; UV (methanol), λ_{max} 396 nm; ^{1}H NMR (500 MHz, $CDCl_3$) δ 7.60 (d, J = 16.0 Hz, 1H, H-7), 7.12 (dd, J = 8.5 and 2.0 Hz, 1H, H-6″), 7.04 (d, J = 2.0 Hz, 1H, H-2″), 7.00 (d, J = 15.5 Hz, 1H, H-1), 6.93 (d, J = 8.5 Hz, 1H, H-5″), 6.64 (d, J = 10.5 Hz, 1H, H-6′), 6.46 (d, J = 16.0 Hz, 1H, H-6), 6.14 (d, J = 10.5 Hz, 1H, H-5′), 5.98 (d, J = 15.5 Hz, 1H, H-2), 5.97 (m, 1H, H-11‴), 5.89 (brs, 1H, 4″-OH), 5.72 (s, 1H, H-4), 5.59 (m, 1H, H-10‴), 4.31 (m, 1H, H-13‴), 4.11 (q, J = 7.0 Hz, 2H, H-1⁗), 3.94 (s, 3H, 3″-OCH_3), 3.17 (s, 3H, 3′-OCH_3), 2.83 (d, J = 7.5 Hz, 1H, H-2′), 2.39 (m, 1H, H-12‴), 2.27 (t, J = 7.5 Hz, 2H, H-2⁗), 2.15 (brd, J = 10.5 Hz, 1H, H-9‴), 1.86 (m, 1H, H-14b‴), 1.59 (m, 2H, H-3‴), 1.50 (m, 1H, H-14a‴), 1.40−1.22 (m, 16H, H-4‴, H-5‴, H-6‴, H-7‴, H-8‴, H-15‴, H-16‴, H-17‴), 1.24 (t, J = 7.0 Hz, 3H, H-2⁗), 0.89 (brt, J = 6.8 Hz, 3H, H-18‴); ^{13}C NMR (125 MHz, $CDCl_3$) δ 190.9 (C-4′), 184.4 (C-5), 181.8 (C-3), 173.8 (C-1‴), 150.0 (C-6′), 148.1 (C-4″), 147.5 (C-1), 146.8 (C-3″), 141.4 (C-7), 135.1 (C-11‴), 134.3 (C-10‴), 128.2 (C-5′), 127.4 (C-1″), 127.4 (C-2), 123.1 (C-6″), 121.4 (C-6), 114.8 (C-5″), 109.6 (C-2″), 101.2 (C-4), 99.8 (C-3′), 84.5 (C-13‴), 60.2 (C-1⁗), 55.9 (3″-OCH_3), 51.1 (3′-OCH_3), 48.9 (C-1′), 47.6 (C-9‴), 46.8 (C-2′), 38.2 (C-12‴), 34.3 (C-2‴), 32.5 (C-14‴), 31.5 (C-16‴), 29.4, 29.3, 29.2, 29.0, 29.0 (C-4‴, C-5‴, C-6‴, C-7‴, C-8‴), 25.1 (C-15‴), 24.9 (C-3‴), 22.5 (C-17‴), 14.2 (C-2⁗), 14.0 (C-18‴).

*Compound **2***: HRMS-FAB (negative) (*m*/*z*) [M − H]$^-$ calcd for $C_{41}H_{53}O_{10}$ 705.3639, found 705.3616; FAB MS (negative), *m*/*z* 705, 557, 477, 455; IR (dry film), ν_{max} 3401 (OH), 1731 (ester CO), 1703 (CO), 1630 (conjugated CO) cm^{-1}; UV (methanol), λ_{max} 396 nm; ^{1}H NMR (500 MHz, $CDCl_3$) δ 7.60 (d, J = 16.0 Hz, 1H, H-7), 7.12 (dd, J = 8.5 and 1.5 Hz, 1H, H-6″), 7.04 (d, J = 2.0 Hz, 1H, H-2″), 7.00 (d, J = 15.7 Hz, 1H, H-1), 6.93 (d, J = 8.5 Hz, 1H, H-5″), 6.64 (d, J = 10.5 Hz, 1H, H-6′), 6.46 (d, J = 16.0 Hz, 1H, H-6), 6.14 (d, J = 10.5 Hz, 1H, H-5′), 5.98 (d, J = 15.7 Hz, 1H, H-2), 5.96 (m, 1H, H-11‴), 5.89 (brs, 1H, 4″-OH), 5.72 (s, 1H, H-4), 5.60 (m, 1H, H-12‴), 4.29 (m, 1H, H-9‴), 4.12 (q, J = 7.0 Hz, 2H, H-1⁗), 3.94 (s, 3H, 3″-OCH_3), 3.17 (s, 3H, 3′-OCH_3), 2.82 (d, J = 7.5 Hz, 1H, H-2′), 2.39 (m, 1H, H-10‴), 2.28 (t, J = 7.5 Hz, 2H, H-2⁗), 2.16 (brd, J = 11.5 Hz, 1H, H-13‴), 1.89 (m, 1H, H-8b‴), 1.60 (m, 2H, H-3‴), 1.50 (m, 1H, H-8a‴), 1.38−1.22 (m, 16H, H-4‴, H-5‴, H-6‴, H-7‴, H-14‴, H-15‴, H-16‴, H-17‴), 1.25 (t, J = 7.0 Hz, 3H, H-2⁗), 0.88 (brt, J = 6.8 Hz, 3H, H-18‴); ^{13}C NMR (125 MHz, $CDCl_3$) δ 190.9 (C-4′), 184.4 (C-5), 181.8 (C-3), 173.9 (C-1‴), 150.1 (C-6′), 148.1 (C-4″), 147.6 (C-1), 146.8 (C-3″), 141.3 (C-7), 134.9 (C-11‴), 134.4 (C-12‴), 128.2 (C-5′), 127.4 (C-2), 127.3 (C-1″), 123.1 (C-6″), 121.4 (C-6), 114.8 (C-5″), 109.6 (C-2″), 101.2 (C-4), 99.8 (C-3′), 84.5 (C-9‴), 60.2 (C-1⁗), 55.9 (3″-OCH_3), 51.2 (3′-OCH_3), 48.9 (C-1′), 47.6 (C-13‴), 46.8 (C-2′), 38.2 (C-10‴), 34.3 (C-2‴), 32.5 (C-8‴), 31.8 (C-16‴), 25.3 (C-7‴), 24.9 (C-3‴), 29.3, 29.1, 29.1, 29.0, 28.8 (C-4‴, C-5‴, C-6‴, C-14‴, C-15‴), 22.6 (C-17‴), 14.2 (C-2⁗), 14.0 (C-18‴).

*Compound **3***: HRMS-FAB (negative) (*m*/*z*) [M − H]$^-$ calcd for $C_{41}H_{53}O_{10}$ 705.3639, found 705.3616; FAB MS (negative), *m*/*z* 705, 577, 455, 427; IR (dry film), ν_{max} 3433 (OH), 1740 (ester CO), and 1625 (conjugated CO) cm^{-1}; UV (methanol), λ_{max} 410 nm; ^{1}H NMR (500 MHz, $CDCl_3$) δ 7.60 (d, J = 16.0 Hz, 1H, H-7), 7.37 (d, J = 16.0 Hz, 1H, H-1), 7.13 (dd, J = 8.0 and 2.0 Hz, 1H, H-6″), 7.05 (d, J = 2.0 Hz, 1H, H-2″), 6.94 (d, J = 8.0 Hz, 1H, H-5″), 6.47 (d, J = 16.0 Hz, 1H, H-6), 6.45 (brdd, J = 6.5 and 2.0 Hz, 1H, H-6′), 6.26 (d, J = 16.0 Hz, 1H, H-2), 5.90 (brs, 1H, 4″-OH), 5.79 (s, 1H, H-4), 5.46 (dt, J = 15.5 and 8.5 Hz, 1H, H-9‴), 5.20 (brdd, J = 15.5 and 8.5 Hz, 1H, H-10‴), 4.36 (brt, J = 6.5 Hz, 1H, H-13‴), 4.12 (q, J = 7.3 Hz, 2H, H-1⁗), 3.95 (s, 3H, 3″-OCH_3), 3.48 (s, 3H, 3′-OCH_3), 3.31 (dd, J = 6.5 and 2.0 Hz, 1H, H-5′), 3.21 (dd, J = 2.5 and 2.0 Hz, 1H, H-2′), 2.85 (dt, J = 8.5 and 2.5 Hz, 1H, H-11‴), 2.28 (t, J = 7.5 Hz, 2H, H-2⁗), 1.94 (brq, J = 6.5 Hz, 2H, H-8‴), 1.64−1.56 (m, 2H, H-3‴), 1.95 (dt, J = 1.0 and 2.5 Hz, 1H, H-12‴), 1.56−1.50 (m, 1H, H-14b‴), 1.42−1.35 (m, 1H, H-14a‴), 1.33−1.22 (m, 14H, H-4‴, H-5‴, H-6‴, H-7‴, H-15‴, H-16‴, H-17‴), 1.25 (t, J = 7.3 Hz, 3H, H-2⁗), 0.88 (brt, J = 7.0 Hz, 3H, H-18‴); ^{13}C NMR (125 MHz, $CDCl_3$) δ

201.7 (C-4′), 185.0 (C-5), 181.1 (C-3), 173.8 (C-1‴), 148.0 (C-4″), 146.8 (C-3″), 141.4 (C-7), 140.8 (C-1′), 136.6 (C-1), 132.4 (C-9‴), 131.6 (C-6′), 130.6 (C-10‴), 127.5 (C-1″), 124.0 (C-2), 123.1 (C-6″), 121.8 (C-6), 114.8 (C-5″), 101.9 (C-4), 109.6 (C-2″), 95.3 (C-3′), 85.1 (C-13‴), 60.2 (C-1⁗), 56.0 (3″-OCH_3), 56.0 (C-5′), 53.6 (3′-OCH_3), 44.0 (C-2′), 41.9 (C-11‴), 41.3 (C-12‴), 34.3 (C-2‴), 32.2 (C-8‴), 31.6 (C-16‴), 29.9 (C-14‴), 29.1, 29.1, 29.0, 28.9 (C-4‴, C-5‴, C-6‴, C-7‴), 25.4 (C-15‴), 24.9 (C-3‴), 22.4 (C-17‴), 14.0 (C-18‴), 14.2 (C-2⁗).

Compound ***4****:* HRMS-FAB (negative) (*m*/*z*) $[M - H]^-$ calcd for $C_{41}H_{53}O_{10}$ 705.3639; found 705.3608; FAB MS (negative), *m*/*z* 705, 577, 455, 427; IR (dry film), ν_{max} 3453 (OH), 1740 (ester CO), and 1625 (conjugated CO) cm^{-1}; UV (methanol), λ_{max} 410 nm; ^1H NMR (500 MHz, $CDCl_3$) δ 7.60 (d, J = 16.0 Hz, 1H, H-7), 7.37 (d, J = 16.0 Hz, 1H, H-1), 7.12 (dd, J = 8.0 and 2.0 Hz, 1H, H-6″), 7.05 (d, J = 2.0 Hz, 1H, H-2″), 6.94 (d, J = 8.0 Hz, 1H, H-5″), 6.48 (d, J = 16.0 Hz, 1H, H-6), 6.45 (brd, J = 6.5 Hz, 1H, H-6′), 6.27 (d, J = 16.0 Hz, 1H, H-2), 5.88 (brs, 1H, 4″-OH), 5.79 (s, 1H, H-4), 5.36 (dt, J = 11.0 and 7.0 Hz, 1H, H-9‴), 5.10 (brt, J = 10.5 Hz, 1H, H-10‴), 4.36 (brt, J = 6.0 Hz, 1H, H-13‴), 4.13 (q, J = 7.0 Hz, 2H, H-1⁗), 3.95 (s, 3H, 3″-OCH_3), 3.48 (s, 3H, 3′-OCH_3), 3.25 (m, 1H, H-2′), 3.24 (m, 1H, H-5′), 3.14 (dt, J = 10.0 and 2.6 Hz, 1H, H-11‴), 2.29 (t, J = 7.5 Hz, 2H, H-2‴), 2.04 (dq, J = 15.0 and 7.5 Hz, 2H, H-8‴), 1.90 (brt, J = 2.6 Hz, 1H, H-12‴), 1.70 (m, 1H, H-14b‴), 1.62 (m, 2H, H-3‴), 1.46−1.22 (m, 1H, H-14a‴), 1.40−1.22 (m, 14H, H-4‴, H-5‴, H-6‴, H-7‴, H-15‴, H-16‴, H-17‴), 1.26 (t, J = 7.5 Hz, 3H, H-2⁗), 0.87 (brt, J = 7.0 Hz, 3H, H-18‴); ^{13}C NMR (125 MHz, $CDCl_3$) δ 201.5 (C-4′), 185.0 (C-5), 181.1 (C-3), 173.8 (C-1‴), 148.1 (C-4″), 146.8 (C-3″), 141.4 (C-7), 140.7 (C-1′), 136.6 (C-1), 131.5 (C-6′), 131.4 (C-9‴), 130.0 (C-10‴), 127.5 (C-1″), 124.1 (C-2), 123.1 (C-6″), 121.8 (C-6), 114.8 (C-5″), 109.6 (C-2″), 101.9 (C-4), 95.3 (C-3′), 84.9 (C-13‴), 60.2 (C-1⁗), 56.0 (3″-OCH_3), 56.0 (C-5′), 53.6 (3′-OCH_3), 44.1 (C-2′), 42.1 (C-12‴), 36.5 (C-11‴), 34.3 (C-2‴), 31.7 (C-16‴), 30.3 (C-14‴), 29.5, 29.2, 29.2, 29.1 (C-4‴, C-5‴, C-6‴, C-7‴), 27.5 (C-8‴), 25.5 (C-15‴), 24.9 (C-3‴), 22.4 (C-17‴), 14.2 (C-2⁗), 14.0 (C-18‴).

Compound ***5****:* HRMS-FAB (negative) (*m*/*z*) $[M - H]^-$ calcd for $C_{41}H_{53}O_{10}$ 705.3639, found 705.3629; FAB MS (negative), *m*/*z* 705, 555, 477, 419, 417; IR (film), ν_{max} 3451 (OH), 1741 (ester CO), and 1625 (conjugated CO) cm^{-1}; UV (methanol), λ_{max} 410 nm; ^1H NMR (500 MHz, $CDCl_3$) δ 7.60 (d, J = 15.5 Hz, 1H, H-7), 7.37 (d, J = 16.0 Hz, 1H, H-1), 7.13 (dd, J = 8.5 and 1.5 Hz, 1H, H-6″), 7.05 (d, J = 1.5 Hz, 1H, H-2″), 6.94 (d, J = 8.5 Hz, 1H, H-5″), 6.47 (d, J = 16.0 Hz, 1H, H-6), 6.45 (brdd, J = 5.9 and 1.5 Hz, 1H, H-6′), 6.26 (d, J = 15.5 Hz, 1H, H-2), 5.90 (brs, 1H, 4″-OH), 5.79 (s, 1H, H-4), 5.47 (dt, J = 15.7 and 6.5 Hz, 1H, H-13‴), 5.20 (brdd, J = 15.5 and 9.5 Hz, 1H, H-12‴), 4.35 (brt, J = 5.5 Hz, 1H, H-9‴), 4.12 (q, J = 7.3 Hz, 2H, H-1⁗), 3.95 (s, 3H, 3″-OCH_3), 3.46 (s, 3H, 3′-OCH_3), 3.31 (dd, J = 6.5 and 2.5 Hz, 1H, H-5′), 3.21 (dd, J = 3.3 and 2.2 Hz, 1H, H-2′), 2.85 (dt, J = 9.5 and 2.6 Hz, 1H, H-11‴), 2.27 (t, J = 7.5 Hz, 2H, H-2‴), 1.95 (dt, J = 1.2 and 3.2 Hz, 1H, H-10‴), 1.93 (brq, J = 6.5 Hz, 2H, H-14‴), 1.78 (m, 1H, H-8b‴), 1.59 (m, 2H, H-3‴), 1.42−1.22 (m, 12H, H-4‴, H-5‴, H-6‴, H-7‴, H-16‴, H-17‴), 1.33−1.22 (m, 2H, H-15‴), 1.30 (m, 1H, H-8a‴), 1.25 (t, J = 7.3 Hz, 3H, H-2⁗), 0.87 (t, J = 7.0 Hz, H-18‴); ^{13}C NMR (125 MHz, $CDCl_3$) δ 201.7 (C-4′), 185.0 (C-5), 181.1 (C-3), 173.8 (C-1‴), 148.0 (C-4″), 146.8 (C-3″), 141.4 (C-7), 140.8 (C-1′), 136.6 (C-1), 132.6 (C-13‴), 131.6 (C-6′), 130.5 (C-12‴), 127.5 (C-1″), 124.0 (C-2), 123.1 (C-6″), 121.8 (C-6), 114.8 (C-5″), 109.6 (C-2″), 101.9 (C-4), 95.3 (C-3′), 85.1 (C-9‴), 60.2 (C-1⁗), 56.0 (3″-OCH_3), 56.0 (C-5′), 53.6 (3′-OCH_3), 44.0 (C-2′), 41.9 (C-11‴), 41.3 (C-10‴), 34.3 (C-2‴), 32.2 (C-14‴), 31.3 (C-16‴), 29.9 (C-8‴), 29.2, 29.0, 29.0, 28.9 (C-4‴, C-5‴, C-6‴, C-15‴), 25.7 (C-7‴), 24.9 (C-3‴), 22.4 (C-17‴), 14.2 (C-2⁗), 14.1 (C-18‴).

Compound ***6****:* HRMS-FAB (negative) (*m*/*z*) $[M - H]^-$ calcd for $C_{41}H_{53}O_{10}$ 705.3639, found 705.3643; FAB MS (negative), *m*/*z* 705, 555, 477, 419, 417; IR (dry film), ν_{max} 3455 (OH), 1740 (ester CO), 1625 (conjugated CO) cm^{-1}; UV (methanol), λ_{max} 410 nm; ^1H NMR (500 MHz, $CDCl_3$) δ 7.60 (d, J = 16.0 Hz, 1H, H-7), 7.36 (d, J = 15.5 Hz, 1H, H-1), 7.13 (dd, J = 8.0 and 2.0 Hz, 1H, H-6″), 7.05 (d, J = 1.5 Hz, 1H, H-2″), 6.94 (d, J = 8.0 Hz, 1H, H-5″), 6.48 (d, J = 16.0 Hz, 1H, H-6), 6.44 (brd, J = 6.5 Hz, 1H, H-6′), 6.27 (d, J = 15.5 Hz, 1H, H-2), 5.88 (brs, 1H, 4″-OH), 5.79 (s, 1H, H-4), 5.37 (dt, J = 10.5 and 7.4 Hz, 1H, H-13‴), 5.10 (brt, J = 11.0 Hz, 1H, H-12‴), 4.35 (brt, J = 6.4 Hz, 1H, H-9‴), 4.17 (q, J = 7.0 Hz, 2H, H-1⁗), 3.95 (s, 3H, 3″-OCH_3), 3.48 (s, 3H, 3′-OCH_3), 3.25 (m, 1H, H-2′), 3.25 (dd, J = 6.3 and 2.6 Hz, 1H, H-5′), 3.14 (dt, J = 10.5 and 2.7 Hz, 1H, H-11‴), 2.27 (t, J = 7.5 Hz, 2H, H-2‴), 2.05 (dq, J = 15.4 and 7.6 Hz, 2H, H-14‴), 1.89 (brt, J = 2.6 Hz, 1H, H-10‴), 1.70 (m, 1H, H-8b‴), 1.60 (m, 2H, H-3‴), 1.40−1.22 (m, 14H, H-4‴, H-5‴, H-6‴, H-7‴, H-15‴, H-16‴, H-17‴), 1.36 (m, 1H, H-8a‴), 1.25 (t, J = 7.0 Hz, 3H, H-2⁗), 0.89 (t, J = 7.0 Hz, 3H, H-18‴); ^{13}C NMR (125 MHz, $CDCl_3$) δ 201.5 (C-4′), 185.0 (C-5), 181.1 (C-3), 173.8 (C-1‴), 148.1 (C-4″), 146.8 (C-3″), 141.4 (C-7), 140.7 (C-1′), 136.6 (C-1), 131.7 (C-6′), 131.5 (C-13‴), 129.9 (C-12‴), 127.5 (C-1″), 124.1 (C-2), 123.1 (C-6″), 121.8 (C-6), 114.8 (C-5″), 109.6 (C-2″), 101.9 (C-4), 95.3 (C-3′), 84.9 (C-9‴), 60.2 (C-1⁗), 56.0 (3″-OCH_3), 55.9 (C-5′), 53.6 (3′-OCH_3), 44.1 (C-2′), 42.2 (C-10‴), 36.5 (C-11‴), 34.3 (C-2‴), 31.5 (C-16‴), 30.3 (C-8‴), 29.3, 29.2, 29.0, 29.0 (C-4‴, C-5‴, C-6‴, C-15‴), 27.5 (C-14‴), 25.8 (C-7‴), 24.9 (C-3‴), 22.6 (C-17‴), 14.3 (C-2⁗), 14.1 (C-18‴).

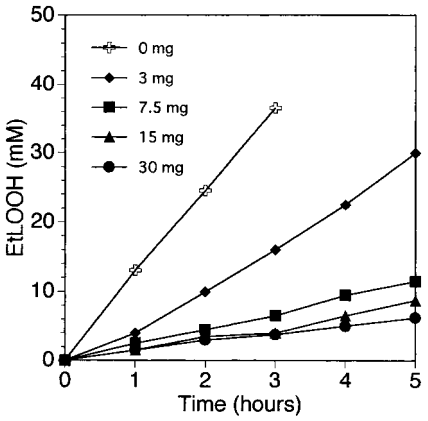

Figure 2. Antioxidant activity of different amounts of curcumin against the oxidation of ethyl linoleate (3 g).

RESULTS AND DISCUSSION

HPLC Analysis of Radical Reaction Products from Curcumin. To observe the antioxidation reaction of curcumin, it should show activity toward oxidation of the surrounding lipid. However, the amount of curcumin relative to that of the lipid should be as low as possible because a higher amount of curcumin would dimerize (*15*). First, we checked the antioxidant activity of different amounts of curcumin to determine the most suitable amount. Figure 2 shows the antioxidant activity of 3−30 mg of curcumin against AIBN-induced ethyl linoleate (3 g) oxidation. Curcumin showed a concentration-dependent inhibition of the accumulation of hydroperoxide. The lowest concentration of curcumin used in this experiment (3 mg) still exhibited antioxidant activity; thus, we employed this amount for analysis of the antioxidant reaction products. The radical oxidation reaction was carried out with 3 mg of curcumin and 3 g of ethyl linoleate in a reaction vial (ca. 1.2 mM curcumin and ca. 1.5 M for ethyl linoleate) at 40 °C, and the reaction products were analyzed by HPLC using a cyanopropylated silica gel (CN) column. The analytical data for the reaction mixture at 2.5 h and the control experiment, which was carried out without ethyl linoleate, are shown in Figure 3. From the data, a new peak was clearly observed at a 6.7 min retention time in the lipid-containing experiment along with a large curcumin peak at 8.4 min. In the control experiment,

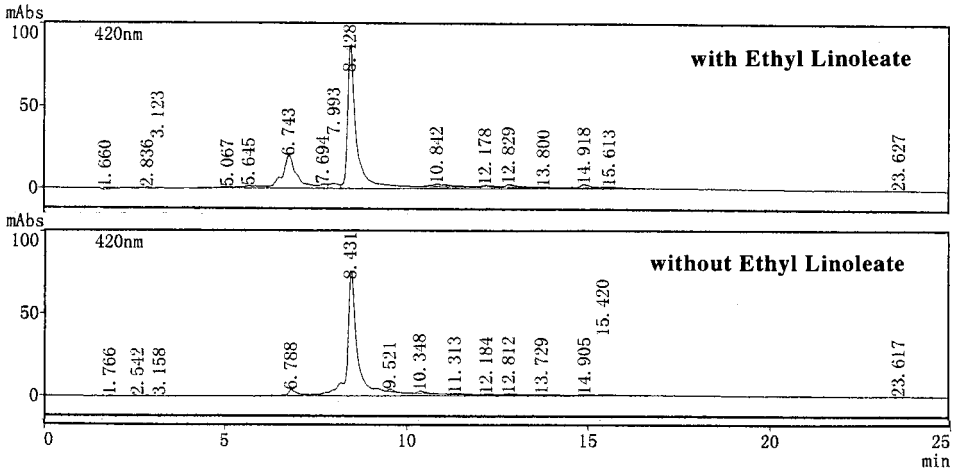

Figure 3. HPLC analytical data of antioxidation process of curcumin (3 mg) with (top) or without (bottom) ethyl linoleate (3 g) The column used was a Develosil CN-5, and detection was at 420 nm.

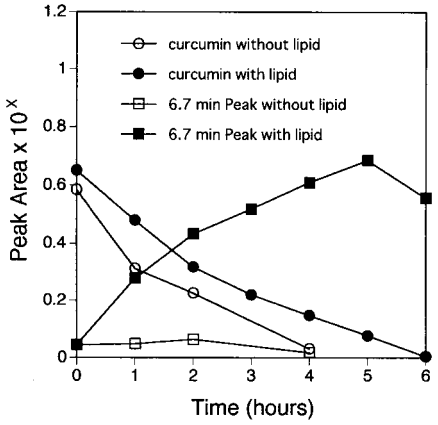

Figure 4. Time course results of peak areas for 6.7 min peak and curcumin's peak obtained by HPLC analysis under both lipidic and nonlipidic conditions. In the scale of the *Y* axis, *x* is −6 for the 6.7 min peak and −7 for the curcumin peak.

the corresponding peak was negligibly small. The time course analysis of the new peak at 6.7 min and the curcumin peak are summarized in Figure 4. The data show that curcumin in both experiments decreased almost continuously, whereas the new 6.7 min peak increased for 5 h only in the lipid-containing experiment. The main products under the lipid-containing conditions were the compounds corresponding to the 6.7 min peak, which were probably produced from both curcumin and ethyl linoleate.

Isolation and Structure Identification of Coupling Products. To clarify that the 6.7 min peak substances were the coupling products of curcumin and the lipid, we isolated them and determined the chemical structures of the substances. One hundred and seventy vials, each of which contained 3 mg of curcumin and 3 g of ethyl linoleate, were incubated at 40 °C for 4 h. After removal of most of the linoleate and AIBN, the reaction mixture was purified by MPLC using the same type of preparative sized column to collect the substances of the 6.7 min peak. An HPLC analysis of the substances collected using a reversed phase column revealed that they mainly consisted of six compounds as shown in Figure 5. These materials were separated again by preparative HPLC, affording pure compounds **1**−**6** in 2.6% total yield from curcumin. Although this isolation yield is very low, it should be noted that this yield does not reflect the real conversion yield because

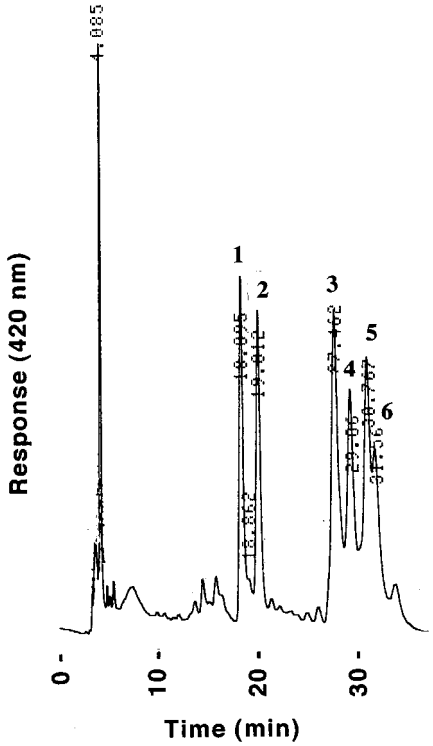

Figure 5. Separation pattern of compounds **1**−**6** by HPLC with an ODS column (solvent, 85% CH_3CN, 16 mL/min; detection, 420 nm).

of unavoidable loss in the multistep purification used. To obtain an accurate conversion yield from curcumin to the coupling compounds, some detailed kinetic studies should be required; however, no other outstanding peak was observed in the HPLC analysis of the reaction mixture even when it was detected by another detection wavelength such as 300 nm (for phenolics) and 360 nm (for conjugated phenolics) (data not shown). Thus, compounds **1**−**6** should be the main conversion products from curcumin under the conditions used.

Compound **1** was isolated as a yellow powder. Its molecular formula was estimated as $C_{41}H_{54}O_{10}$ from the negative FAB MS result [*m/z* 705.3651 $(M - H)^-$]. The molecular formula indicated that **1** was an oxidative coupling product consisting of curcumin, ethyl linoleate, and molecular oxygen. In the ^1H NMR of **1**, both signal sets due to the original curcumin and ethyl linoleate were observed; however, several signals assignable to

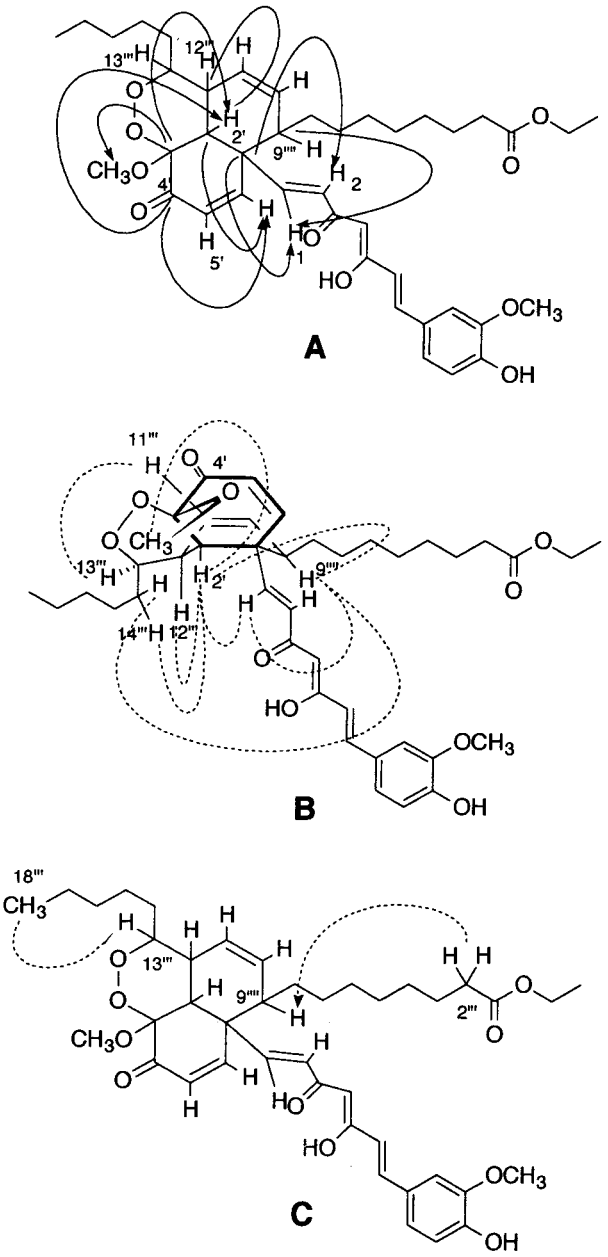

Figure 6. Selected carbon−proton long-range connectivities observed in HMBC (arrows in A), NOE correlations observed in NOESY (dashed lines in B), and proton−proton correlations observed in TOCSY (dashed arrows in C) of compound **1**.

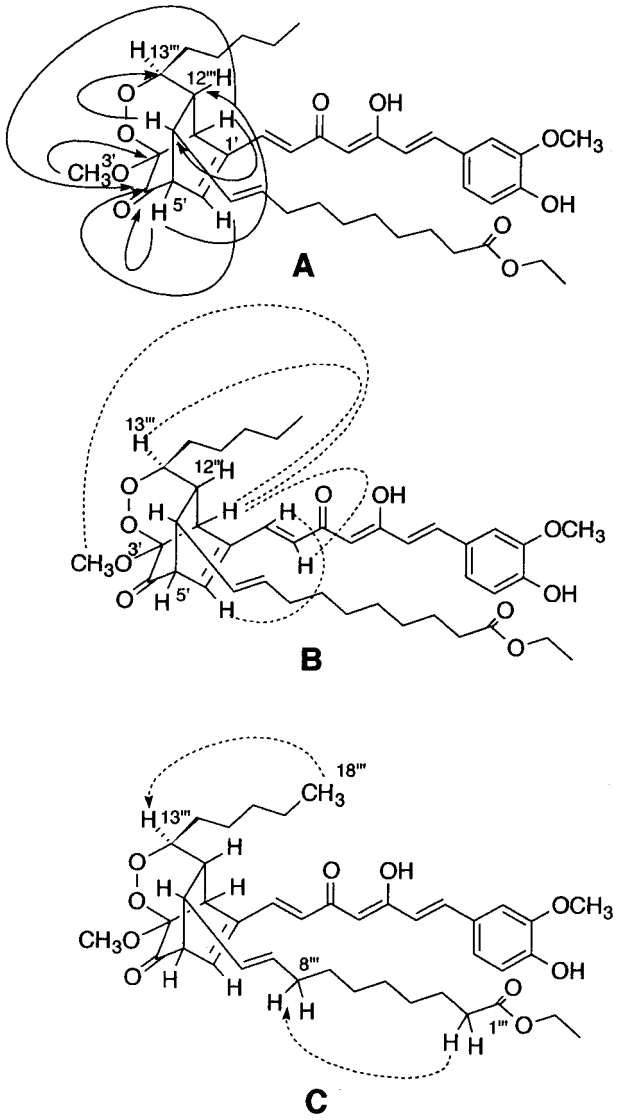

Figure 7. Selected carbon−proton long-range connectivities observed in HMBC (arrows in A), NOE correlations observed in NOESY (dashed lines in B), and proton−proton correlations observed in TOCSY (dashed arrows in C) of compound **3**.

the aromatic part of curcumin and the olefinic part of the linoleate had disappeared, indicating that the double bond of the linoleate reacted with the aromatic part of curcumin. The fine structure of the coupled moiety of **1** was elucidated mainly by the 2D NMR technique. Analysis of the proton−proton couplings observed in the COSY spectrum and C−H long-range coupling connectivities around the coupled moiety in the HMBC spectrum revealed a tricyclic structure including a carbonyl group at the 4′-position (δ 190.9, ν_{max} 1703 cm^{-1}) and two olefins at the 5′- and 10‴-positions (Figure 6A). There should be an oxygen function between C13‴ and C3′ on the basis of their carbon chemical shift values (C13‴, δ 84.5; C3′, δ 99.8). Consideration of the oxygen count of the molecular formula and a slight downfield shift of the C13‴ signal with that of the normal monooxygenated carbon indicated that a peroxyl group should exist between the two carbons at the 13‴- and 3′-positions (*18*). The stereochemistry of the tricyclic ring system was deduced by the NOE correlations. The phase-sensitive NOESY spectrum of **1** showed five important correlations, which were observed from H2′ to H1, H9‴, H12‴, H14‴, and the 3′-methoxyl group, respectively, indicating that the protons at the 2′-, 9‴-, and 12‴-positions, the alkyl substituents at the 1′- and 13‴-positions, and the methoxyl group at the 3′-position should have the same α-orientation, as illustrated in Figure 6B. Finally, two kinds of groups attached to the tricyclic system at the 9‴- and 13‴-positions were elucidated. From the chemical structure of the starting ethyl linoleate, these should be pentyl and ethoxycarbonylheptyl groups. Although the proton and carbon signals due to the alkyl chains of both groups did not separate sufficiently for the determination of the attached position; a TOCSY spectrum of **1** (mixing time = 0.12 s) enabled the position to be determined. In this spectrum, clear correlations between the 18‴-methyl protons and the 13‴-proton and between the 2‴-proton and the 9‴-proton were observed as illustrated in Figure 6C, which indicated that the pentyl group was attached at the 13‴-position and the ethoxycarbonylheptyl group

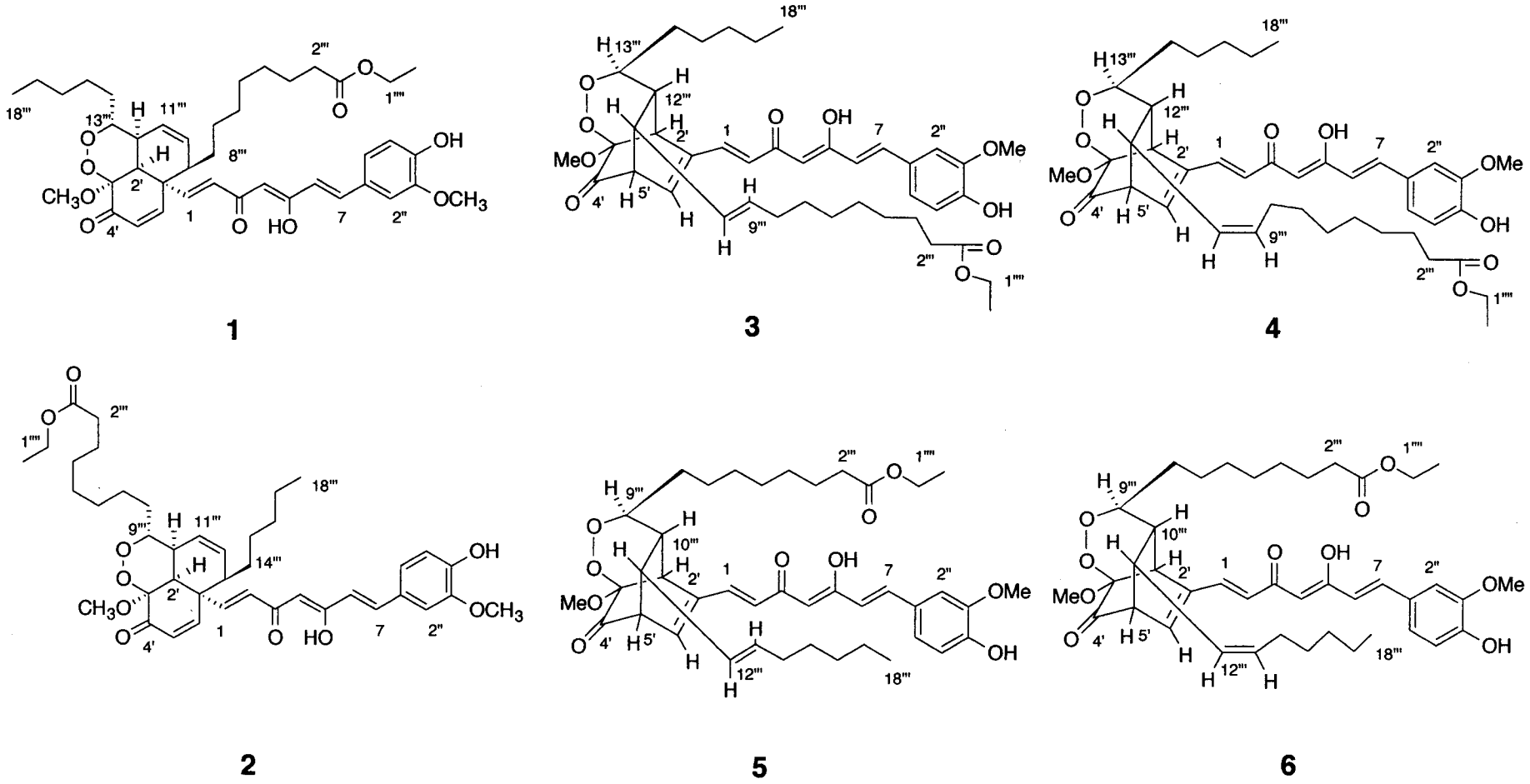

Figure 8. Chemical structures of compounds **1**−**6**. Tentative position numberings are given on the basis of the numbering system of starting curcumin and ethyl linoleate.

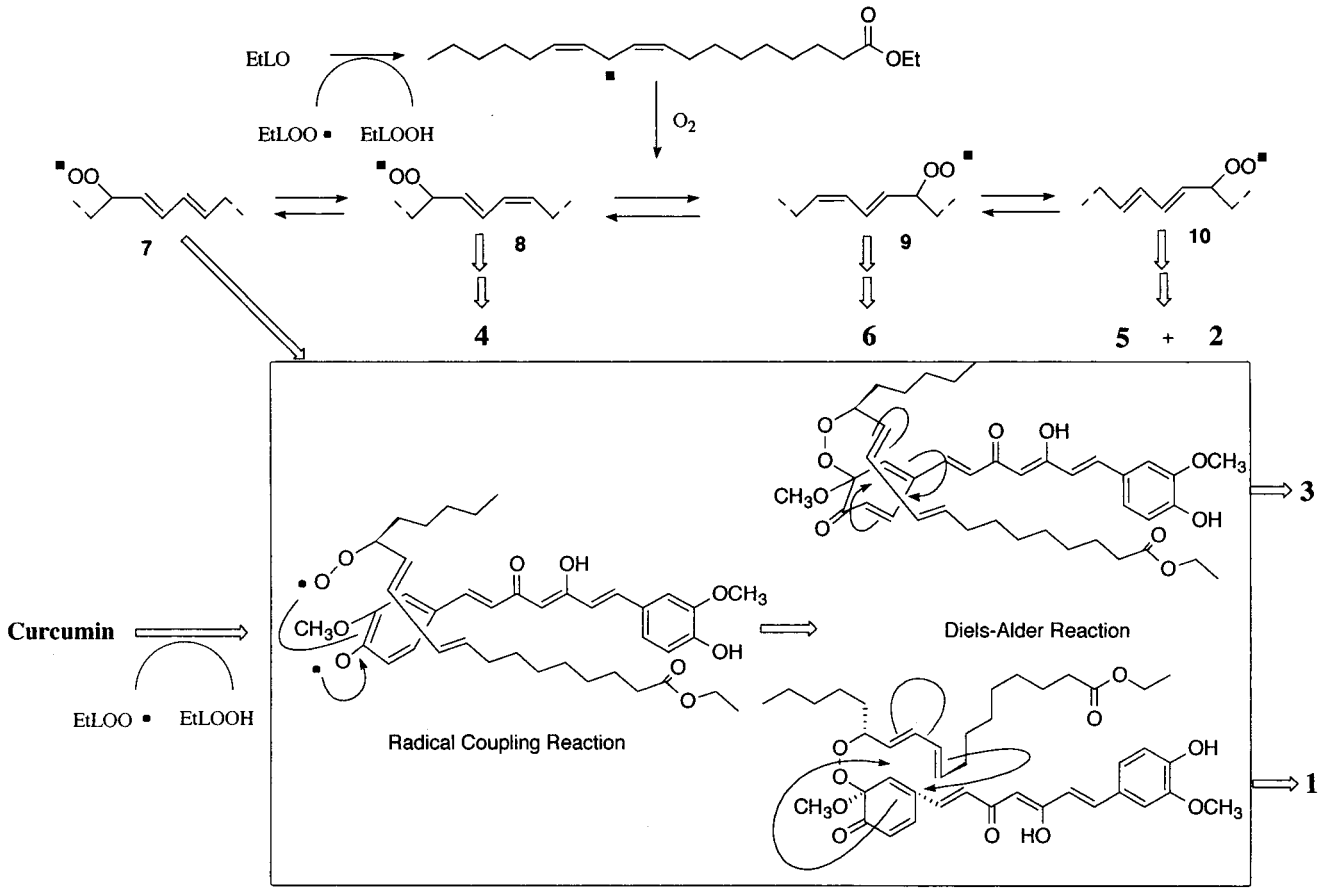

Figure 9. Proposed mechanism for antioxidation of curcumin against a polyunsaturated lipid (ethyl linoleate) oxidation. EtLO, EtLOOH, and EtLOO• represent ethyl linoleate, ethyl linoleate hydroperoxide, and ethyl linoleate hydoperoxyl radical, respectively.

at the 9‴-position of the tricyclic ring systems. Thus, the structure of compound **1** was established as depicted in Figure 8.

Compound **2** was isolated as a yellow powder. Its molecular formula was $C_{41}H_{54}O_{10}$, as determined by a pseudo-molecular ion peak in negative FAB MS [*m*/*z* 705.3616 $(M - H)^-$]. Spectroscopic analysis including UV, IR, and ^1H and ^{13}C NMR gave almost the same results as those of compound **1**. Only the fragmentation pattern was different from that of **1**. These results strongly indicated that **2** was isomeric with **1** at the positions of the alkyl chain groups attached to the same tricyclic system. Thus, the TOCSY spectrum was measured to determine the positions of these alkyl substituents. In fact, the TOCSY spectrum of **2** showed opposite correlations between the 2‴-proton and the 9‴-proton and between the 18‴-protons and the 13‴-proton, respectively, to those of **1**. Thus, compound **2** was determined to have structure **2**, as depicted in Figure 8.

Compound **3** was also isolated as a yellow powder, and its molecular formula was determined to be $C_{41}H_{54}O_{10}$ from the FAB MS results [*m*/*z* 705.3616 $(M - H)^-$]. Its spectroscopic data appeared to be different from those of **1** and **2**. However, an intensive analysis of the ^1H NMR data revealed that both signal sets due to one of the benzene rings of curcumin and due to an olefin from the linoleate had disappeared, similar to those of compounds **1** and **2**. From a proton−proton coupling connectivity in H2′−H12‴−H11‴−H5′−H6′ found in the COSY spectrum and six H−C long-range coupling connectivities in the HMBC spectrum, a bicyclo[2.2.2] structure was revealed (Figure 7A). The presence of a slightly downfield shifted monooxygenated carbon (C13‴, δ 85.1) and acetalic carbon (C3′, δ 95.3) and the oxygen count of the molecular formula strongly indicated that a peroxyl group should exist between C13‴ and C3′ and suggested the new tricyclic system as depicted. The stereochemistry around the tricyclic system was deduced by the proton coupling constants and NOE correlations (Figure 7B). The phase-sensitive NOESY spectrum of **3** showed a strong correlation between H2′ and H13‴, suggesting that H13‴ had the axial orientation in the conformationally restricted 1,2-dioxycyclohexane ring. The stereochemistry of H12‴ and H11‴ was also deduced to be trans by the small coupling constant (J = 2.5 Hz) of the two protons. The groups attached to the tricyclic ring system at the 11‴- and 13‴-positions were elucidated. A trans olefin was determined to be adjacent to the 11‴-position by the chemical shift of H11‴ (δ 2.85). At the other end of the olefin (9‴-position) and at the 13‴-position, the remaining alkyl groups must be attached. These groups should be pentyl and ethoxycarbonylheptyl groups on the basis of the starting ethyl linoleate structure. To determine the attached groups, a TOCSY spectrum was measured, which showed clear connectivities from the 18‴-methyl proton to the H13‴ and from the α-protons of the ethyl ester to the olefinic protons at the 9‴-position, clarifying that the pentyl group was attached to the 13‴-position and the esteric alkyl chain to the 9‴-position (Figure 7C). The compound therefore has the structure **3** as shown in Figure 8 (*19*).

Compound **4** was isolated as a yellow powder, and its molecular formula was determined to be $C_{41}H_{54}O_{10}$ from the FAB MS [*m*/*z* 705.3608 $(M - H)^-$]. All spectroscopic

data including the mass fragmentation pattern were very similar to those of **3**; however, only the NMR signal sets due to an olefin were different. The coupling constant ($J = 10.5$ Hz) between the protons on the olefin indicated that the geometry of the olefin should be cis, which was supported by the slightly upfield-shifted adjacent carbons (C8‴, δ 27.5; C11‴, δ 36.5) compared with those of **3**. The 2D NMR data of **4** including HMBC, NOESY, and TOCSY gave the same analytical results as those of **3**, indicating that the remainder of **4** was the same as **3**. Thus, **4** was the cis-olefinic isomer of **3** as illustrated in Figure 8.

Compounds **5** and **6** were isolated as yellow powders, and their molecular formulas were both determined to be $C_{41}H_{54}O_{10}$ from each FAB MS result [*m/z* 705.3629 $(M - H)^-$ for **5** and 705.3643 $(M - H)^-$ for **6**]. The spectroscopic data (UV, IR, and ^1H and ^{13}C NMR) of **5** and **6**, except for the mass fragmention pattern, gave almost the same results as those of **3** and **4**, respectively, which indicated that a similar structural relationship existed between **3** and **5** and between **4** and **6**, as was observed between compounds **1** and **2**. The TOCSY spectrum of **4** showed the opposite substitution pattern of the two alkyl groups on the tricyclic system to that of **3**, and the spectrum of **5** also showed a similar opposite pattern to that of **4**. Thus, compounds **5** and **6** were determined to be the corresponding isomeric compounds of the substitution of the alkyl chain groups on the tricyclic system to **3** and **4**, respectively. Thus, they have structures **5** and **6** as depicted in Figure 8.

Antioxidant Mechanism of Curcumin in the Presence of Linoleate. From our elucidation of the chemical structures of the six isolated compounds, we propose the antioxidant mechanism of curcumin in the presence of ethyl linoleate as illustrated in Figure 9. As shown in Figure 9, curcumin traps a radical at the phenolic group and is converted to a curcumin radical. The curcumin radical reacts with a peroxyl radical of the ethyl linoleate at the 3′-position, affording a coupling product through a peroxyl linkage. The coupling product is not very stable because the aromatic stability of the original benzene ring is disrupted by the coupling reaction. Thus, the subsequent Diels−Alder reaction occurs smoothly in the coupling product. It is accepted that linoleic acid gives four isomeric peroxyl radicals during its autoxidation (*20*), which were presumed by the chemical structures of the corresponding four hydroperoxides including the 9-*trans*-11-*trans*-diene 13-hydroperoxide, 9-*cis*-11-*trans*-diene 13-hydroperoxide, 10-*trans*-12-*cis*-diene 9-hydroperoxide, and 10-*trans*-12-*trans*-diene 9-hydroperoxide. Coupling of the isomeric peroxyl radical **7** with the curcumin radical at the 3′-position would produce the corresponding peroxide. The unstable peroxide could then be converted by the intramolecular Diels−Alder reaction. Reaction of the double bond at the 11-position of linoleate part of the peroxide with the conjugated diene from the 1′,5′-position of the curcumin would afford compound **3**. On the other hand, reaction of the double bond at the 1′-position of the curcumin part with the diene from the linoleate part would give compound **1**. By similar reaction procedures, compounds **2** and **5** would be produced from the peroxyl radical **10**, compound **4** from the peroxyl radical **8**, and compound **6** from the peroxyl radical **9**, respectively. It is predictable that one of the two types of the Diels−Alder reactions, as illustrated in Figure 9, does not occur in the case of the peroxides derived from the peroxyl radicals **8** and **9**, because an alkyl substituent on the cis-double bond of the linoleate part of the peroxides prevents the reaction due to its steric hindrance.

It is apparent from the structure of the isolated compounds that curcumin shows a chain-breaking antioxidant activity with the termination reaction by the coupling of $A^•$ and $X^•$. When curcumin exists in the presence of an unsaturated lipid, the lipid hydroperoxyl radical acts as $X^•$ and forms several isomeric hydroperoxides by coupling reaction. The hydroperoxides then react intramolecularly to produce and accumulate the characteristic tricyclic compounds in the system.

ACKNOWLEDGMENT

We thank Dr. Tokuzo Kawase, Osaka City University, for IR measurements. We also thank the Central Instrument Center of the Faculty of Pharmaceutical Science of the University of Tokushima for MS measurements and the Cooperative Center of the University of Tokushima for opportunities to record 1D NMR spectra.

Supporting Information Available: Six tables of correlation data of COSY, NOESY, HMBC, and TOCSY of compounds **1**−**6**. This material is available free of charge via the Internet at http://pubs.acs.org.

LITERATURE CITED

(1) Govindarajan. V. S. Turmeric-chemistry, technology, and quality. *CRC Crit. Rev. Food Sci. Nutr.* **1980**, *12*, 199−246.

(2) Ruby, A. J.; Kuttan, G.; Babu, K. D. Anti-tumor and antioxidant activity of natural curcuminoids. *Cancer Lett.* **1995**, *94*, 79−83.

(3) Sreejayan, R. M. N. Curcuminoids as potent inhibitors of lipid peroxidation. *J. Pharm. Pharmacol.* **1994**, *46*, 1013−1016.

(4) Kelloff, G. J.; Crowell, J. A.; Hawk, E. T.; Steele, V. E.; Lubet, R. A.; Boone, C. W.; Covey, J. M.; Doody, L. A.; Omenn, G. S.; Greenwald, P.; Hong, W. K.; Parkinson, D. R.; Bagheri, D.; Baxter, G. T.; Blunden, M.; Doelts, M. K.; Eisenhauer, K. M.; Johnson, K.; Knapp, G. G.; Longfellow, D. G.; Malone, W. F.; Nayfield, S. G.; Sefried, H. E.; Swall, L. M., Sigman, C. C. Strategy and planning for chemopreventive drug development: clinical development plans II. *J. Cell. Biochem.* **1996**, *26S*, 54−71.

(5) Toda, S.; Miyase, T.; Arichi, H.; Tanizawa, H.; Takino, Y. Natural antioxidants III, antioxidative components isolated from rhizomes of *Curcuma longa. Chem. Pharm. Bull.* **1985**, *33*, 1725−1728.

(6) Uehara, S.; Yasuda, I.; Akiyama, K.; Morita, H.; Takeya, K.; Itokawa, H. Diarylheptanoids from the rhizomes of *Curcuma xanthorrhiza* and *Alpinia officinarum*. *Chem. Pharm. Bull.* **1987**, *35*, 3298−3304.

(7) Masuda, T.; Isobe, J.; Jitoe, A.; Nakatani, N. Antioxidative curcuminoids from rhizomes of *Curcuma xanthorrhiza*. *Phytochemistry* **1992**, *31*, 3645−3647.

(8) Masuda, T.; Jitoe, A.; Isobe, J.; Nakatani, N. Antioxidative and antiinflammatory curcumin-related phenolics from rhizomes of *Curcuma domestica*. *Phytochemistry* **1993**, *32*, 1557−1560.

(9) Masuda, T.; Jitoe, A. Antioxidative and antiinflammatory compounds from tropical gingers: isolation, structure determination, and activities of cassumunins A, B, and C, new complex curcuminoids from *Zingiber cassumunar*. *J. Agric. Food Chem.* **1994**, *42*, 1850−1856.

(10) Masuda, T.; Jitoe, A.; Mabry, T. J. Isolation and structure determination of cassumunarins A, B, and C, new antiinflammatory antioxidants from a tropical ginger, *Zingiber cassumunar*. *J. Am. Oil Chem. Soc.* **1995**, *72*, 1053−1057.
(11) Noguchi, N.; Komuro, E.; Niki, E.; Willson, R. L. Action of curcumin as an antioxidant against lipid peroxidation. *J. Jpn. Oil Chem. Soc.* **1994**, *43*, 1045−1051.
(12) Khopde, S. M.; Priyadarsini, K. I.; Venkatesan, P.; Rao, M. N. A. Free radical scavenging ability and antioxidant efficiency of curcumin and its substituted analogue. *Biophys. Chem.* **1999**, *80*, 85−91.
(13) Jovanoic, S. V.; Steenken, S,; Boone, C. W.; Simic, G. H-atom transfer is a preferred antioxidant mechanism of curcumin. *J. Am. Chem. Soc.* **1999**, *121*, 9677−9681.
(14) Frankel, E. N. *Lipid Oxidation*; The Oily Press: Dundee, Scotland, 1998; pp 129−160.
(15) Masuda, T.; Hidaka, K.; Shinohara, A.; Maekawa, T.; Takeda, Y.; Yamaguchi, H. Chemical studies on antioxidant mechanism of curcuminoid: analysis of radical reaction products from curcumin. *J. Agric. Food Chem.* **1999**, *47*, 71−77.
(16) Pabon, H. J. J. A synthesis of curcumin and related compounds. *Recl. Trav. Chim. Pays-Bas* **1964**, *83*, 379−385.
(17) Terao, J.; Matsushita, A. Products formed by photosensitized oxidation of unsaturated fatty acid esters. *J. Am. Oil Chem. Soc.* **1977**, *54*, 234−238.
(18) Kusumi, K.; Ohtani, I.; Inouye, Y.; Kakisawa, H. Absolute configurations of cytotoxic marine cembranolides; consideration of Mosher's method, *Tetrahedron Lett.* **1988**, *29*, 4731−4734.
(19) Masuda, T.; Bando, H.; Maekawa, T.; Takeda, Y.; Yamaguchi, H. A novel radical terminated compound produced in the antioxidation process of curcumin against oxidation of a fatty acid ester. *Tetrahedron Lett.* **2000**, *41*, 2157−2160.
(20) Frankel, E. N. *Lipid Oxidation*; The Oily Press: Dundee, Scotland, 1998; pp 26−29.

Received for review November 30, 2000. Revised manuscript received February 20, 2001. Accepted February 21, 2001. This study was financially supported by a Grant-in-Aid for Scientific Research from Japan Society of the Promotion of Sciences and by a grant from Kiei-kai Research Foundation (Tokyo).

JF001442X